Mitochondrial damage activates the NLRP10 inflammasome

Eicke Latz (eicke.latz@uni-bonn.de)
University of Bonn https://orcid.org/0000-0003-1488-5666

Tomasz Próchnicki
University of Bonn, Institute of Innate Immunity

Matilde B. Vasconcelos
University of Bonn https://orcid.org/0000-0003-1487-6495

Matthew Mangan
University of Bonn, Institute of Innate Immunity

Kim Robinson
A*STAR Skin Research Labs

Sarah Rösing
Technische Universität Dresden, Department of Dermatology

Fraser Duthie
Institute of Innate Immunity, Medical Faculty, University of Bonn

Lena Standke
University of Bonn, Institute of Innate Immunity https://orcid.org/0000-0003-3113-125X

Romina Kaiser
Institute of Innate Immunity

Maximilian Rothe
University Hospital Bonn https://orcid.org/0000-0002-9749-1293

Dagmar Wachten
University of Bonn, Institute of Innate Immunity

Claudia Günther
Technische Universität Dresden, Department of Dermatology

Thomas Kufer
University of Hohenheim, Institute for Nutritonal Medicine https://orcid.org/0000-0003-4563-0412

Franklin Zhong
Nanyang Technological University https://orcid.org/0000-0002-0516-6021

Letter

Keywords:

Posted Date: February 4th, 2022

DOI: https://doi.org/10.21203/rs.3.rs-1295136/v1

Title: Mitochondrial damage activates the NLRP10 inflammasome

Authors: Tomasz Próchnicki[1,2], Matilde B. Vasconcelos[1†], Matthew S. J. Mangan[1,3†], Kim S. Robinson[4,5], Sarah Rösing[6], Fraser G. Duthie[1], Lena Standke[1], Romina Kaiser[1], Maximilian Rothe[1], Dagmar Wachten[1], Claudia Günther[6], Thomas A. Kufer[7], Franklin L. Zhong[8,9], Eicke Latz[1,3,10*]

Affiliations:

[1]Institute of Innate Immunity, Medical Faculty, University of Bonn; Bonn, 53127, Germany.
[2]IFM Therapeutics, Boston, MA, 02116, USA.
[3]German Center of Neurodegenerative Diseases (DZNE); Bonn, 53127, Germany.
[4]A*STAR Skin Research Labs (A*SRL), Clinical Sciences Building; Singapore, 308232, Singapore.
[5]Skin Research Institute of Singapore (SRIS), Clinical Sciences Building; Singapore, 308232, Singapore.
[6]Department of Dermatology, Medical Faculty Carl Gustav Carus, Technische Universität Dresden; Dresden, 01307, Germany.
[7]Institute of Nutritional Medicine, Department of Immunology, University of Hohenheim, Stuttgart; Stuttgart, 70593, Germany.
[8]Skin Research Institute of Singapore (SRIS), Immunos; Singapore, 138648, Singapore.
[9]Lee Kong Chian School of Medicine, Nanyang Technological University; Singapore, 308232, Singapore.
[10]Division of Infectious Diseases and Immunology, Department of Medicine, University of Massachusetts Medical School; Worcester, MA, 01655, USA.

[†]These authors contributed equally to this work.
*Corresponding author. Email: eicke.latz@uni-bonn.de

Abstract: Upon detecting pathogens or cell stress, several NOD-like receptors (NLRs) form inflammasome complexes with the adaptor ASC and caspase-1, inducing activation of IL-1β and IL-18, and gasdermin D-dependent cell death. The triggers and activation mechanisms of several inflammasome-forming sensors remain poorly understood. Here, we found that mitochondrial damage activates the NLRP10 inflammasome, leading to ASC speck formation and caspase-1-dependent cytokine release. Unlike AIM2, NLRP10 monitors mitochondrial integrity in a mitochondrial DNA-independent manner, suggesting the detection of distinct molecular entities displayed by the damaged organelles. NLRP10 is highly expressed in differentiated human keratinocytes, where it also senses mitochondrial damage. Our study reveals a novel inflammasome that surveils mitochondrial integrity, which could lead to further understanding of inflammatory diseases.

One-Sentence Summary: NLRP10 senses mitochondrial damage and forms an inflammasome in a mitochondrial DNA-independent manner.

Main Text:

Inflammasomes are protein complexes that bridge the recognition of pathogens and sterile cell damage to gasdermin D-mediated pyroptotic cell death and initiate IL-1β-driven inflammation (*1*). Due to aging and metabolic dysfunction or gain-of-function mutations, chronic inflammasome activation can contribute to a broad spectrum of inflammatory diseases (*2*). Therefore, members of this family of innate immune receptors represent possible targets for pharmacological intervention (*3*).

Most inflammasome-forming sensors belong to the NACHT, LRR, and PYD domain-containing (NLRP) protein family. Their LRR domains take part in recognizing perturbations of key cellular processes and microbe- or stress-associated ligands (*4*). The roles of several NLRP family members and the signals that activate them are incompletely characterized, impeding our understanding of disease pathogenesis and productive drug development.

We examined inflammasome activation by *m*-3M3FBS, a reported PLC agonist (*5*) that has been linked to activation of the NLRP3 inflammasome (*6*, *7*). We confirmed that *m*-3M3FBS treatment leads to an inflammasome-driven response in an ASC- and caspase-1-dependent manner (Fig. 1A and fig. S1, A and B) but found no evidence that this process is mediated by NLRP3 (Fig. 1B and fig. S1, C-G), in contrast to the canonical NLRP3 activator nigericin. Expression of NLRP10, but not other NLRP proteins, enabled ASC speck formation in *m*-3M3FBS-treated HEK cells with a fluorescent ASC reporter (Fig. 1C). This NLRP10-mediated inflammasome response was specific to *m*-3M3FBS, as nigericin and the AIM2 inflammasome activator poly-(dA:dT) did not cause ASC speck formation in NLRP10 reporter cells (fig. S2).

To determine the upstream signal for NLRP10 activation, we tracked the subcellular localization of fluorescently tagged NLRP10. NLRP10 was a soluble cytosolic protein in resting cells, but it translocated to punctate structures in *m*-3M3FBS-treated cells (Fig. 1D). These puncta partially colocalized with the mitochondrial marker TOMM20 (Fig. 1E) but not with other organelle markers (fig. S3). Scanning transmission electron microscopy of *m*-3M3FBS-treated cells revealed profound morphological changes of mitochondria (Fig. 1F), consistent with mitochondrial permeability transition (mPT) (*8*). This damage was reflected by cytosolic leakage of mitochondrial matrix-targeted mCherry reporter (Fig. 1G), whose subcellular distribution showed a rapid loss of granularity, which coincided with NLRP10-driven ASC speck formation (Fig. 1H). Notably, the mitochondrial events and NLRP10 activation in *m*-3M3FBS-stimulated cells were not linked to Ca^{2+} fluxes (fig. S4).

m-3M3FBS-induced mitochondrial rupture and inflammasome activation also occurred in macrophages (Fig. 2A), which do not express NLRP10 (*9*-*12*), suggesting that another sensor is involved. Indeed, we found that, in this cell type, *m*-3M3FBS triggers AIM2 (Fig. 2B). Furthermore, two other mitochondria-targeting molecules, thapsigargin (Fig. 2B and fig. S5, A-C) (*13*) and SMBA1 (fig. S5, D and E) (*14*), triggered AIM2 inflammasome activation in macrophages. In agreement with their mitochondria-damaging activity, thapsigargin and SMBA1 also elicited NLRP10 translocation to TOMM20-positive mitochondria and induced NLRP10-driven ASC speck formation in HEK cells (fig. S5, F and G).

It was previously shown that AIM2 can sense mitochondrial DNA (mtDNA) (*15*). Consistently, *m*-3M3FBS- and thapsigargin-mediated AIM2 activation depended on mtDNA in macrophages (Fig. 2C and fig. S6A). In contrast, *m*-3M3FBS- and thapsigargin-driven NLRP10 activation was independent of mtDNA in NLRP10-expressing AIM2-deficient macrophages (Fig. 2C), suggesting a new mechanism for the detection of mitochondrial damage. These data were corroborated in HEK cells expressing NLRP10 (fig. S6, B and C).

We next assessed the mechanism by which the NLRP10 and AIM2 inflammasome-inducing agents damage mitochondria. We determined that the mPT inhibitor cyclosporin A (CsA) (*13*, *16*-*18*) selectively blocked mitochondrial rupture and AIM2 inflammasome activation in thapsigargin- and SMBA1- but not *m*-3M3FBS-treated macrophages (Fig. 2D and fig. S7, A and B). Similarly, CsA blocked mitochondrial damage and NLRP10-mediated ASC speck formation in HEK cells (Fig. 2E and fig. S7, C and D). These findings suggest that NLRP10 and AIM2 are activated by distinct molecular events downstream of mitochondrial damage. The protection from mitochondrial damage coincided with inhibition of ASC speck formation and IL-1β release (fig. S8, A-C), corroborating that mitochondrial damage triggers AIM2 and NLRP10 activation. Lastly, Debio025 and NIM811, non-immunosuppressive CsA analogs with specific mitoprotective activity profiles (*19*, *20*), also inhibited inflammasome responses to thapsigargin, but not to *m*-3M3FBS (fig. S8, D-I).

Confirming NLRP10 as an inflammasome-forming sensor, NLRP10 colocalized with ASC in *m*-3M3FBS- and thapsigargin-treated cells, but not under resting conditions (Fig. 3A). Neither individually expressed PYD or NACHT domains nor Walker A and B mutants of NLRP10 (*21*) enabled inflammasome activation (Fig. 3B), demonstrating that the NLRP10-mediated inflammasome response required expression of the full-length protein. Since NLRP10 lacks an LRR domain, this suggests that the NLRP10 NACHT domain can sense the molecular entities that are exposed or produced upon mitochondrial damage. Moreover, AIM2- and NLRP10-driven IL-1β secretion was blocked by the caspase-1 inhibitor VX-765 (Fig. 3C), indicating that the NLRP10 inflammasome engages caspase-1.

NLRP10 is highly expressed in the skin epidermis (*22*-*24*). We confirmed that NLRP10 mRNA is selectively enriched in terminally differentiated keratinocytes in the *stratum granulosum* (*24*) (Fig. 4A). In keeping with this observation, immortalized N/TERT keratinocytes, which represent the stem/progenitor compartment of the epidermis, did not display pyroptotic cell death morphology (Fig. 4B) or secrete cleaved IL-1β after *m*-3M3FBS treatment (Fig. 4C). This is consistent with low NLRP10 expression at the endogenous level. NLRP10 overexpression in N/TERT cells was sufficient to induce pyroptosis (Fig. 4B) and other hallmarks of inflammasome activation in response to *m*-3M3FBS, including the formation of ASC specks and the release of mature IL-1β (Fig. 4C and D).

Next, we found that $CaCl_2$-driven *in vitro* differentiation of primary human keratinocytes led to a strong increase in NLRP10 mRNA expression (Fig. 4E). In line with this observation, N/TERT keratinocyte differentiation resulted in overall higher levels of IL-1β released upon *m*-3M3FBS stimulation (Fig. 4F). Western blotting analysis confirmed that $CaCl_2$-induced keratinocyte differentiation induces NLRP10 protein expression and enables mature IL-1β secretion in response to *m*-3M3FBS (Fig. 4G). Correspondingly, thapsigargin treatment led to formation of NLRP10 puncta in differentiated primary human keratinocytes (Fig. 4H).

Our study demonstrated that NLRP10 nucleates inflammasomes in cells treated with *m*-3M3FBS, thapsigargin, or SMBA1. In contrast to earlier reports suggesting an inflammasome-inhibitory role for NLRP10 (*25*, *26*), which is the only NLRP family member lacking the LRR domain (*27*), we found that NLRP10 is a novel sensor of mitochondrial damage. Our results also emphasize the capacity of AIM2 to recognize mitochondrial disruption and mtDNA cytosolic leakage (*15*).

NLRP10 variants have been associated with an increased risk of atopic dermatitis (AD) (*28*, *29*). Therefore, it will be important to address whether the inflammasome-forming activity of NLRP10 is linked to its role in AD pathogenesis. In further support of the pathophysiological importance of NLRP10, a study by Zheng *et al.* (2021) (*30*), co-submitted with our work, uncovered a protective role of NLRP10 inflammasome activation in colitis. Given the reported involvement of NLRP10 in regulating innate immune signaling and transcription of inflammatory molecules (*10*, *22*, *23*), it will be interesting to examine under which conditions NLRP10 behaves as an inflammasome and when it exerts other functions, and how this distinction is made. Understanding the partial redundancy between NLRP10 and AIM2 as sensors of mitochondrial damage, especially in *in vivo* studies, will be vital for dissecting the individual roles of AIM2 and NLRP10 in host defense against microbes or sterile inflammatory processes. Such studies will likely reveal pathological disease mechanisms in which targeting of NLRP10 may provide a therapeutic benefit.

References:

1. P. Broz, V. M. Dixit, Inflammasomes: mechanism of assembly, regulation, and signalling. *Nat Rev Immunol*. **16**, 407–420 (2016).
2. L. Broderick, D. De Nardo, B. S. Franklin, H. M. Hoffman, E. Latz, The Inflammasomes and Autoinflammatory Syndromes. *Annu. Rev. Pathol. Mech. Dis.* **10**, 395–424 (2015).
3. M. S. J. Mangan *et al.*, Targeting the NLRP3 inflammasome in inflammatory diseases. *Nat Rev Drug Discov*. **17**, 588–606 (2018).
4. A. Liston, S. L. Masters, Homeostasis-altering molecular processes as mechanisms of inflammasome activation. *Nat Rev Immunol*. **17**, 208–214 (2017).
5. Y.-S. Bae *et al.*, Identification of a Compound That Directly Stimulates Phospholipase C Activity. *Mol Pharmacol*. **63**, 1043–1050 (2003).
6. G.-S. Lee *et al.*, The calcium-sensing receptor regulates the NLRP3 inflammasome through Ca2+ and cAMP. *Nature*. **492**, 123–127 (2012).
7. M. Rossol *et al.*, Extracellular Ca2+ is a danger signal activating the NLRP3 inflammasome through G protein-coupled calcium sensing receptors. *Nat Comms*. **3**, 1329 (2012).
8. H. Friberg, M. Ferrand-Drake, F. Bengtsson, A. P. Halestrap, T. Wieloch, Cyclosporin A, but not FK 506, protects mitochondria and neurons against hypoglycemic damage and implicates the mitochondrial permeability transition in cell death. *J Neurosci*. **18**, 5151–5159 (1998).
9. M. Lech, A. Avila-Ferrufino, V. Skuginna, H. E. Susanti, H.-J. Anders, Quantitative expression of RIG-like helicase, NOD-like receptor and inflammasome-related mRNAs in humans and mice. *International Immunology*. **22**, 717–728 (2010).
10. K. Lautz *et al.*, NLRP10 enhances Shigella-induced pro-inflammatory responses. *Cell Microbiol*. **14**, 1568–1583 (2012).
11. S. Nakajima *et al.*, Characterization of Innate and Adaptive Immune Responses in PYNOD-Deficient Mice. *IH*. **2**, 129–141 (2018).

12. M. Vacca *et al.*, NLRP10 Enhances CD4+ T-Cell-Mediated IFNγ Response via Regulation of Dendritic Cell-Derived IL-12 Release. *Front. Immunol.* **8**, 373 (2017).
13. P. Korge, J. N. Weiss, Thapsigargin directly induces the mitochondrial permeability transition. *European Journal of Biochemistry*. **265**, 273–280 (1999).
14. M. Xin *et al.*, Small-molecule Bax agonists for cancer therapy. *Nat Comms*. **5**, 727 (2014).
15. E. V. Dang, J. G. McDonald, D. W. Russell, J. G. Cyster, Oxysterol Restraint of Cholesterol Synthesis Prevents AIM2 Inflammasome Activation. *Cell*. **171**, 1057–1071.e11 (2017).
16. C. P. Baines *et al.*, Loss of cyclophilin D reveals a critical role for mitochondrial permeability transition in cell death. *Nature*. **434**, 658–662 (2005).
17. E. Basso *et al.*, Properties of the Permeability Transition Pore in Mitochondria Devoid of Cyclophilin D. *Journal of Biological Chemistry*. **280**, 18558–18561 (2005).
18. T. Nakagawa *et al.*, Cyclophilin D-dependent mitochondrial permeability transition regulates some necrotic but not apoptotic cell death. *Nature*. **434**, 652–658 (2005).
19. A. Billich *et al.*, Mode of action of SDZ NIM 811, a nonimmunosuppressive cyclosporin A analog with activity against human immunodeficiency virus (HIV) type 1: interference with HIV protein-cyclophilin A interactions. *J. Virol.* **69**, 2451–2461 (1995).
20. J. Paeshuyse *et al.*, The non-immunosuppressive cyclosporin DEBIO-025 is a potent inhibitor of hepatitis C virus replicationin vitro. *Hepatology*. **43**, 761–770 (2006).
21. J. A. MacDonald, C. P. Wijekoon, K.-C. Liao, D. A. Muruve, Biochemical and structural aspects of the ATP-binding domain in inflammasome-forming human NLRP proteins. *IUBMB Life*. **65**, 851–862 (2013).
22. N. Mirza, A. S. Sowa, K. Lautz, T. A. Kufer, NLRP10 Affects the Stability of Abin-1 To Control Inflammatory Responses. *The Journal of Immunology*. **202**, 218–227 (2018).
23. A. Damm, N. Giebeler, J. Zamek, P. Zigrino, T. A. Kufer, Epidermal NLRP10 contributes to contact hypersensitivity responses in mice. *Eur. J. Immunol.* (2016), doi:10.1002/eji.201646401.
24. J. Lachner, V. Mlitz, E. Tschachler, L. Eckhart, Epidermal cornification is preceded by the expression of a keratinocyte-specific set of pyroptosis-related genes. *Sci. Rep.* **7**, 107 (2017).
25. Y. Wang *et al.*, PYNOD, a novel Apaf-1/CED4-like protein is an inhibitor of ASC and caspase-1. *International Immunology*. **16**, 777–786 (2004).
26. T. Kinoshita, Y. Wang, M. Hasegawa, R. Imamura, T. Suda, PYPAF3, a PYRIN-containing APAF-1-like Protein, Is a Feedback Regulator of Caspase-1-dependent Interleukin-1β Secretion. *Journal of Biological Chemistry*. **280**, 21720–21725 (2005).
27. E. Meunier, P. Broz, Evolutionary Convergence and Divergence in NLR Function and Structure. *Trends in Immunology*. **38**, 744–757 (2017).
28. N. Tanaka *et al.*, Eight novel susceptibility loci and putative causal variants in atopic dermatitis. *J Allergy Clin Immunol*. **148**, 1293–1306 (2021).
29. T. Hirota *et al.*, Genome-wide association study identifies eight new susceptibility loci for atopic dermatitis in the Japanese population. *Nat. Genet.* **44**, 1222–1226 (2012).
30. D. Zheng *et al.*, Epithelial NLRP10 inflammasome mediates protection against intestinal autoinflammation. *Submitted to Nature Immunology* (2022).

Acknowledgments: We would like to thank Dr. Hannes Beckert, Dr. Gabor L. Horvath, Dr. Lydia Maus, and Pia Stausberg from the Microscopy Core Facility of the Medical Faculty at the University of Bonn for providing help, services, and devices funded by the Deutsche Forschungsgemeinschaft (DFG, German Research Foundation) – Projektnummer 13123509 and 169331223. This work was also supported by the Light Microscopy Facility, a Core Facility of the CMCB Technology Platform at TU Dresden. We thank Dr. Damien Bertheloot, Dr. Dominic De Nardo, Dr. Yonatan Herzig, Marta Lovotti, Brian G. Monks, Rainer Stahl, Dr. Lucas Secchim Ribeiro, Gudrun Engels, and Petro Leka (all from the Institute of Innate Immunity in Bonn) for providing reagents and expertise as well as Nick Zimmermann from the Department of Dermatology, Medical Faculty Carl Gustav Carus, Technische Universität Dresden for the outstanding technical assistance.

Funding:

Deutsche Forschungsgemeinschaft (DFG, German Research Foundation) grant EXC2151 (Project-ID 390873048) under Germany's Excellence Strategy (EL)

Deutsche Forschungsgemeinschaft (DFG, German Research Foundation) grant TRR237 (Project-ID 369799452/404458960) (EL, CG)

Deutsche Forschungsgemeinschaft (DFG, German Research Foundation) grant SFB1403 (Project-ID 414786233) (EL)

National Research Foundation-Prime Minister's office, Republic of Singapore: NRF Fellowship 2018 (FLZ)

Nanyang Technological University: NAP2018 (FLZ)

Author contributions:

Conceptualization: TP, MSJM, DW, EL
Writing – original draft: TP, EL
Writing – review & editing: TP, MBV, MSJM, KSR, SR, DW, TAK, FLZ, EL
Methodology: TP, MBV, MSJM, KSR, SR, FGD, LS, RK, MR, TAK
Investigation: TP, MBV, KSR, SR, CG, FLZ, EL
Visualization: TP, MBV, EL
Funding acquisition: CG, FLZ, EL

Competing interests: The authors declare no conflicts of interest. EL is co-founder and consultant of IFM Therapeutics and Odyssey Therapeutics as well as a co-founder and board member of Dioscure Therapeutics.

Data and materials availability: All data are available in the main text or the supplementary materials.

Supplementary Materials
Materials and Methods
Figs. S1 to S8
References (*30*–*45*)

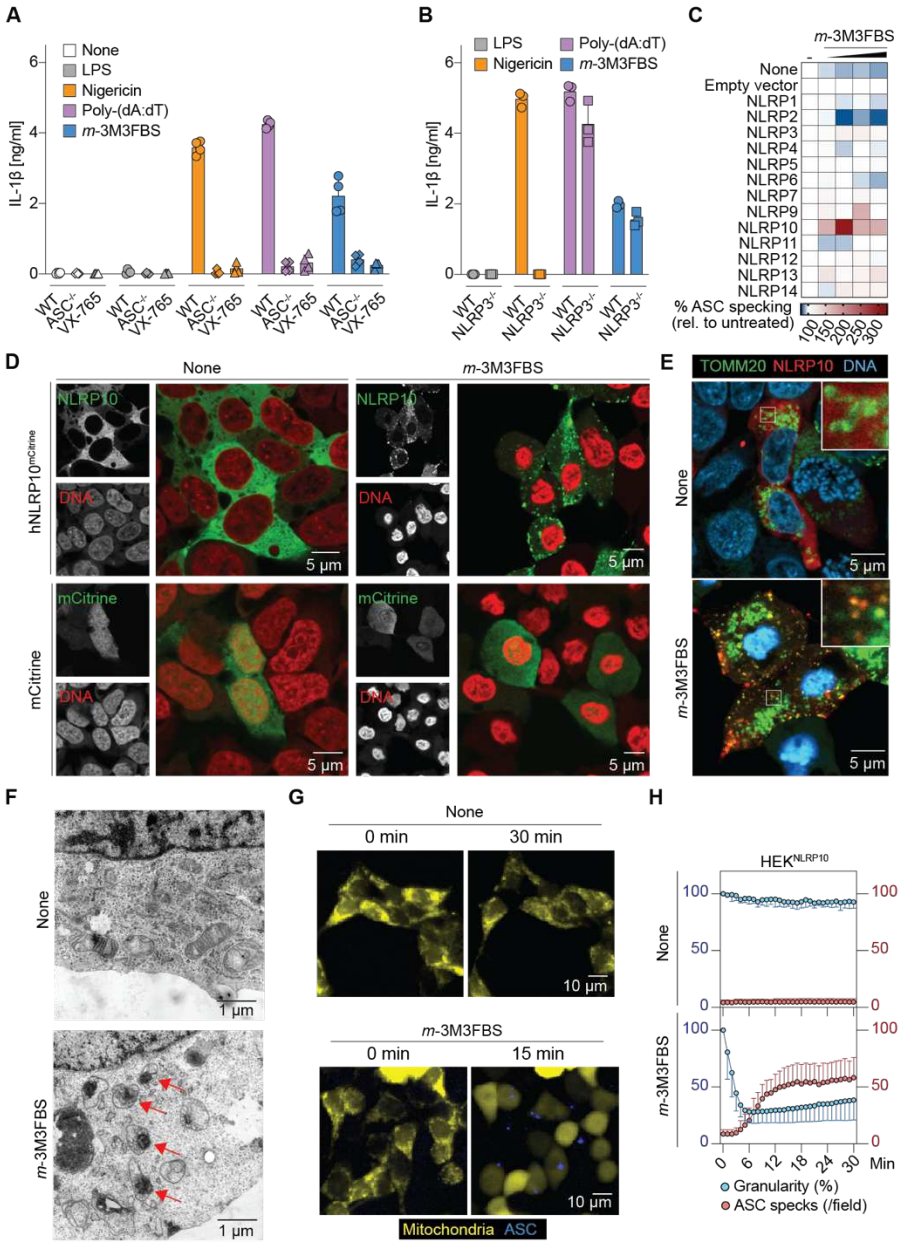

Fig. 1. *m*-3M3FBS triggers mitochondrial damage and NLRP10 inflammasome activation. (**A**) IL-1β secretion from WT, ASC-deficient, or VX-765-pretreated (40 µM) bone marrow-derived macrophages (BMDMs), primed with LPS (200 ng/ml) and stimulated with nigericin (10 µM), poly-(dA:dT) dsDNA (2 µg/ml) or *m*-3M3FBS (85 µM). (**B**) IL-1β secretion from WT or NLRP3-deficient BMDMs, stimulated as in (A). (**C**) ASC speck formation of ASC^{TagBFP} HEK cells expressing an empty vector (EV) or human NLRP1-7, 9-14, stimulated with increasing doses of *m*-3M3FBS (40, 55, 70, or 85 µM). Data normalized to the untreated control. (**D**) Confocal microscopy of HEK cells expressing NLRP10^{mCitrine} or mCitrine as a separate polypeptide, with or without *m*-3M3FBS (85 µM) treatment. (**E**) Confocal microscopy of HEK cells stably expressing NLRP10^{mCherry} and transfected with TOMM20^{mCitrine} mitochondrial marker, with or without *m*-3M3FBS (85 µM) treatment. (**F**) Electron microscopy of HEK cells, with or without *m*-3M3FBS (85 µM) treatment. (**G**) Time-lapse microscopy of HEK cells expressing NLRP10, ASC^{TagBFP} and mCherry targeted to the mitochondrial matrix (using cytochrome c oxidase subunit 8

mitochondrial targeting sequence), with or without *m*-3M3FBS (85 μM) treatment. Images of the same field at treatment onset (0 min) or indicated time points. (**H**) Quantification of mitochondrial fluorescence signal granularity and ASC specks per imaging field. N = 2-4 independent experiments; individual data points (where applicable) are means of technical duplicates or triplicates; all error bars represent SD.

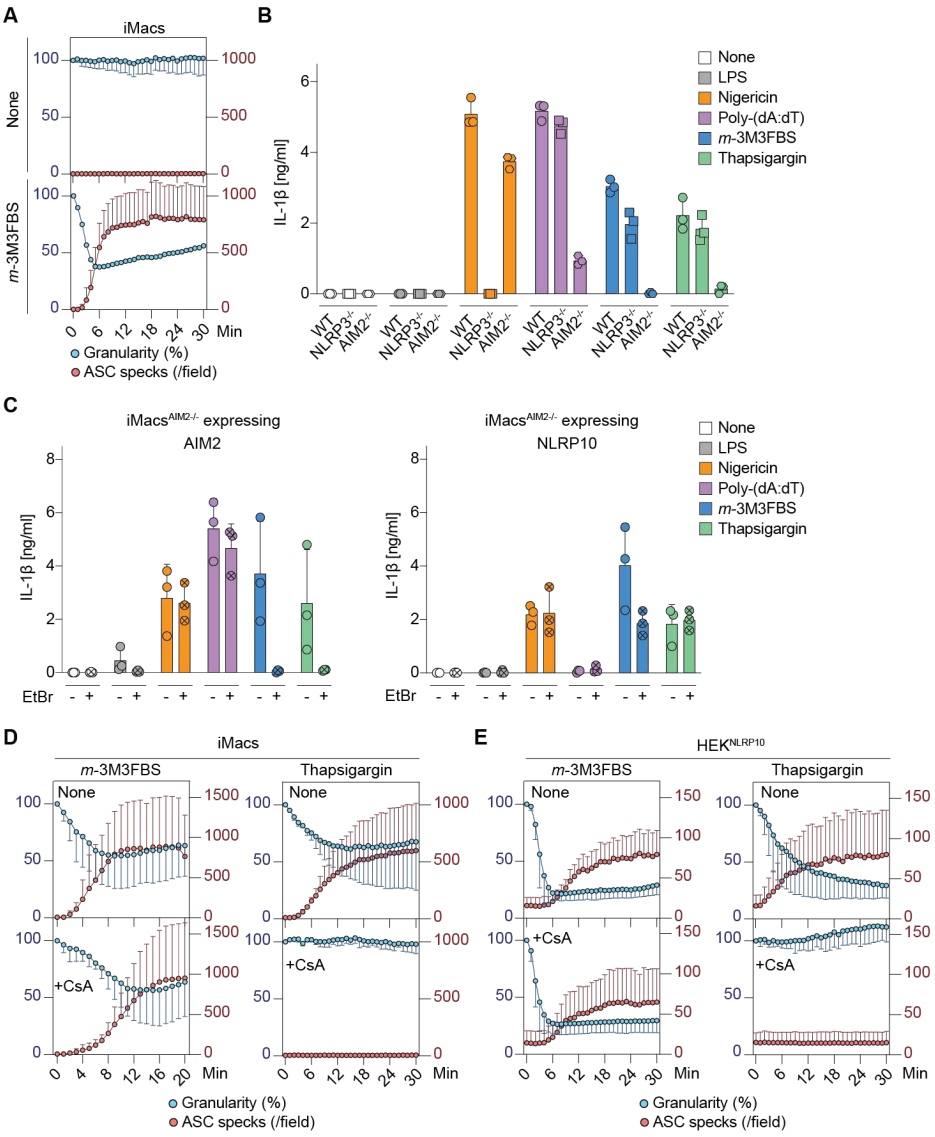

Fig. 2. Mitochondrial permeability transition activates NLRP10 and AIM2 inflammasomes. (**A**) Quantification of mitochondrial fluorescence signal granularity and ASC specks per imaging field, based on time-lapse microscopy of iMacs expressing NLRP3, ASC^{mCerulean} and mCitrine targeted to the mitochondrial matrix (using cytochrome c oxidase subunit 8 mitochondrial targeting sequence), with or without *m*-3M3FBS (85 μM) treatment. (**B**) IL-1β secretion from WT, NLRP3- or AIM2-deficient BMDMs, primed with LPS (200 ng/ml) and stimulated with nigericin (10 μM), poly-(dA:dT) dsDNA (2 μg/ml), *m*-3M3FBS (72 μM) or thapsigargin (20 μM). (**C**) IL-1β secretion from iMacs$^{AIM2-/-}$ overexpressing AIM2 or NLRP10, with or without ethidium bromide (EtBr) (75 ng/ml) pre-treatment to deplete mtDNA, LPS-primed and stimulated as in (B). (**D, E**) Quantification of mitochondrial fluorescence signal granularity and ASC specks per imaging field, based on time-lapse microscopy of iMacs expressing NLRP3, ASC^{mCerulean} and mCitrine targeted to the mitochondrial matrix (D) or HEK cells expressing NLRP10, ASC^{TagBFP} and mCherry targeted to the mitochondrial matrix (E). Cells were treated with *m*-3M3FBS (85 μM) or thapsigargin (20 μM), with or without cyclosporin A (CsA; 15 μM) pre-treatment. N = 3-4 independent experiments; individual data points (where applicable) are means of technical duplicates or triplicates; all error bars represent SD.

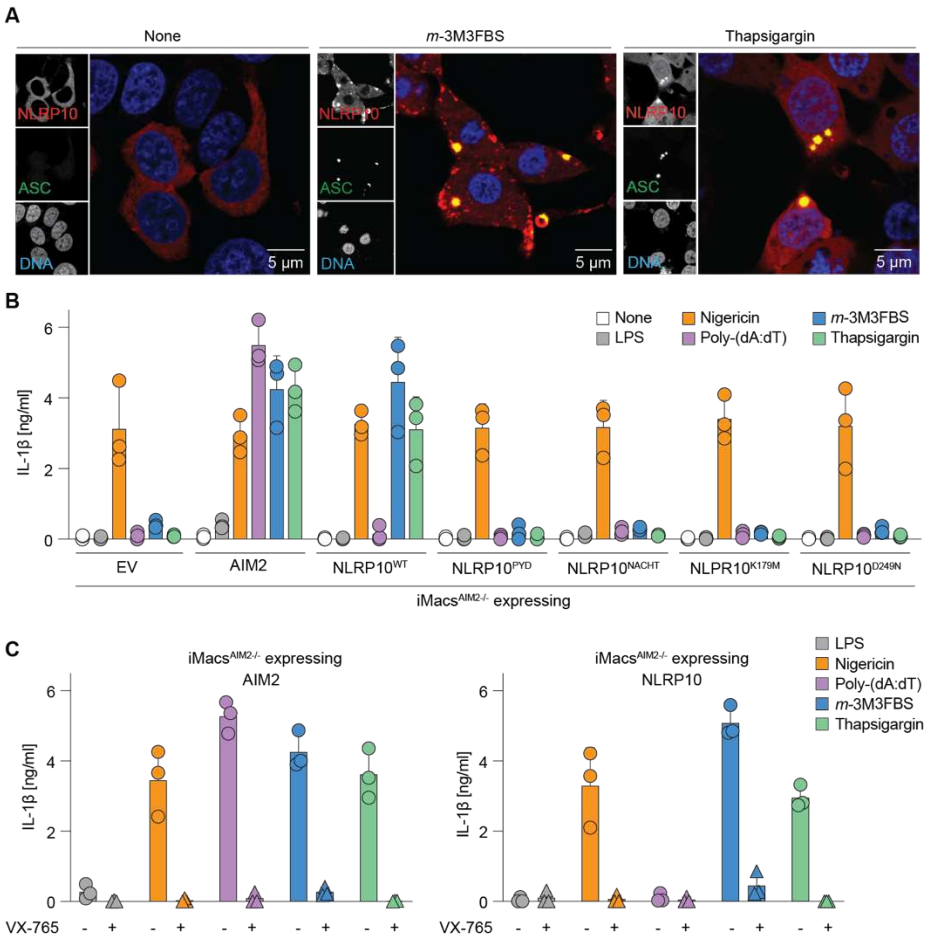

Fig. 3. NLRP10 engages ASC and caspase-1 to trigger a canonical inflammasome response. (**A**) Confocal microscopy of HEK cells expressing NLRP10^{mCherry} and ASC^{mCerulean}, with or without *m*-3M3FBS (85 µM) or thapsigargin (20 µM) treatments. (**B**) IL-1β secretion from iMacs$^{AIM2-/-}$ expressing an empty vector (EV), AIM2, NLRP10 (WT), the NLRP10 PYD or NACHT domains, or Walker A (K179M) or B (D249N) mutants of NLRP10. Cells were LPS-primed (200 ng/ml) and stimulated with nigericin (10 µM), poly-(dA:dT) dsDNA (2 µg/ml), *m*-3M3FBS (85 µM) or thapsigargin (20 µM). (**C**) IL-1β secretion from iMacs$^{AIM2-/-}$ expressing AIM2 or NLRP10, with or without VX-765 (25 µM) pre-treatment, LPS-primed and stimulated as in (B). N = 3 independent experiments; individual data points (where applicable) are means of technical duplicates/triplicates; all error bars represent SD.

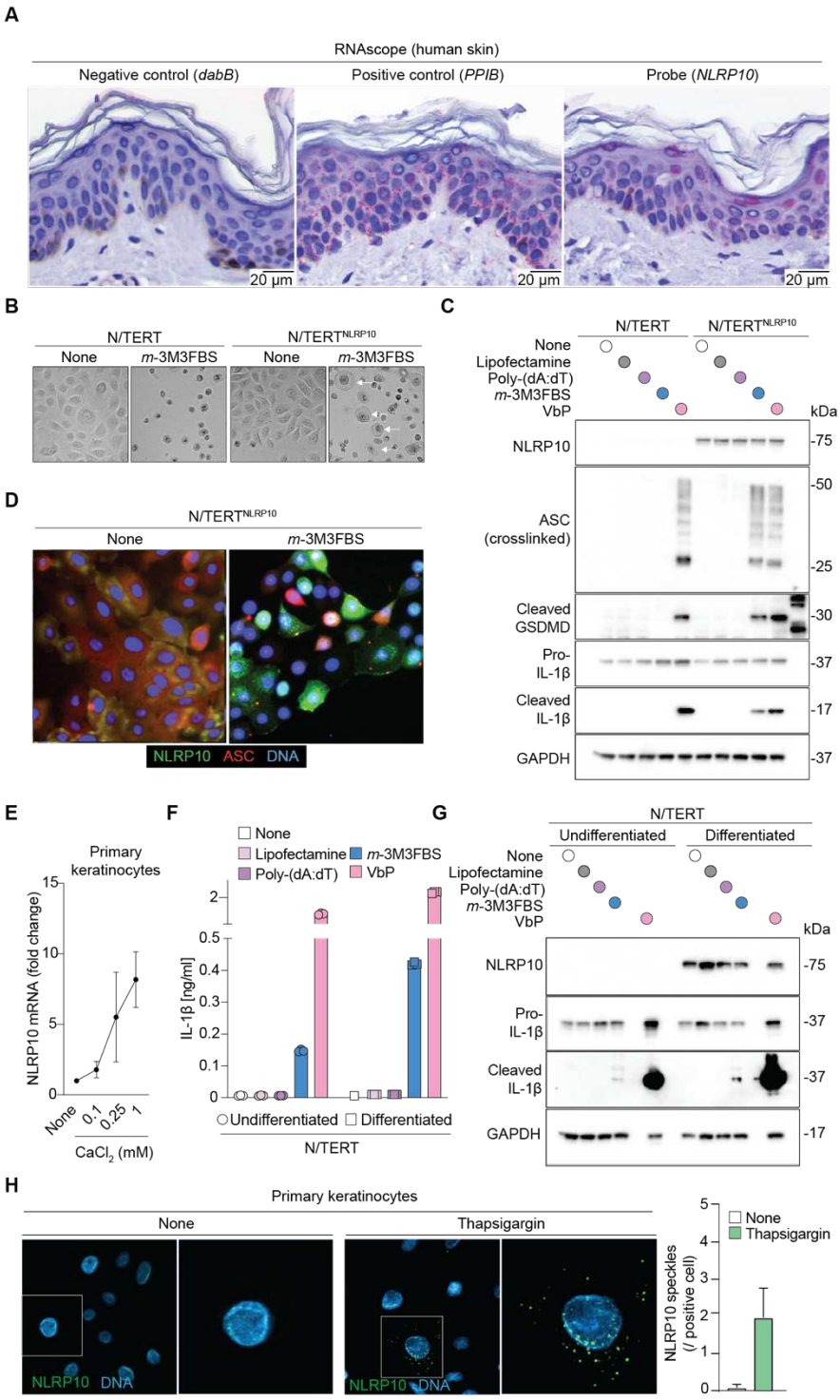

Fig. 4. Keratinocyte differentiation drives NLRP10 expression, enabling responses to mitochondrial damage.

(**A**) RNAscope analysis of human skin stained for dabB (bacterial argininosuccinate lyase; negative control), PPIB (peptidyl-prolyl cis-trans isomerase B; positive control) or NLRP10. Note that positive RNAscope signal appears as pink puncta. Brown staining is caused by endogenous skin pigmentation and should not be confused with positive mRNA signals. (**B**) Phase-contrast microscopy of immortalized N/TERT human keratinocytes, with or without NLRP10 overexpression, with or without *m*-3M3FBS (50 µM) treatment. Cells with pyroptotic morphology

are indicated by arrows. (**C**) Western blot analysis of NLRP10 levels, ASC oligomerization, gasdermin D (GSDMD) cleavage, pro-IL-1β expression, and mature IL-1β release in immortalized N/TERT human keratinocytes, with or without NLRP10 overexpression, stimulated with the NLRP1 activator Val-boroPro (VbP) (3 μM), the NLRP10 activator *m*-3M3FBS (80 μM) or the AIM2 agonist poly-(dA:dT) dsDNA (2 μg/ml). (**D**) Immunofluorescence microscopy of ASC and NLRP10 in immortalized N/TERT human keratinocytes overexpressing NLRP10, with or without *m*-3M3FBS (80 μM) treatment. (**E**) qPCR analysis of NLRP10 mRNA expression in primary human keratinocytes, undifferentiated or differentiated for 6 days in medium containing $CaCl_2$ (0.1-1 mM). (**F**) IL-1β secretion from undifferentiated or differentiated immortalized N/TERT human keratinocytes, stimulated as in (C). (**G**) Western blot analysis of NLRP10 and pro-IL-1β expression, and mature IL-1β release in undifferentiated or differentiated immortalized N/TERT human keratinocytes, stimulated as in (C). (**H**) Immunofluorescence staining, confocal microscopy, and NLRP10 speckles quantification of differentiated primary human keratinocytes, with or without thapsigargin (20 μM) treatment. N = 2-3 independent experiments; individual data points (where applicable) are means of technical duplicates; all error bars represent SD.

Supplementary Files

This is a list of supplementary files associated with this preprint. Click to download.

- FINALNISupplement.pdf